PCCP

Accepted Manuscript

This is an *Accepted Manuscript*, which has been through the Royal Society of Chemistry peer review process and has been accepted for publication.

Accepted Manuscripts are published online shortly after acceptance, before technical editing, formatting and proof reading. Using this free service, authors can make their results available to the community, in citable form, before we publish the edited article. We will replace this *Accepted Manuscript* with the edited and formatted *Advance Article* as soon as it is available.

You can find more information about *Accepted Manuscripts* in the Information for Authors.

Please note that technical editing may introduce minor changes to the text and/or graphics, which may alter content. The journal's standard Terms & Conditions and the Ethical guidelines still apply. In no event shall the Royal Society of Chemistry be held responsible for any errors or omissions in this *Accepted Manuscript* or any consequences arising from the use of any information it contains.

ROYAL SOCIETY OF CHEMISTRY

www.rsc.org/pccp

Journal Name RSCPublishing

ARTICLE

Sequential "click" functionalization of mesoporous titania for energy-relay dye enhanced dye-sensitized solar cells

Cite this: DOI: 10.1039/x0xx00000x

Received 00th January 2012, Accepted 00th January 2012

DOI: 10.1039/x0xx00000x

www.rsc.org/

Eva L. Unger,*[a]† Samuel J. Fretz,[b] Bogyu Lim,[a] George Y. Margulis,[a] Michael D. McGehee[a] and T. Daniel P. Stack*[b]

Energy relay dyes (ERDs) have been investigated previously as a mean to achieve panchromatic spectral response in dye-sensitized solar cells via energy transfer. To reduced the distance between the ERDs and energy-accepting injection dyes (ID) on the surface of a mesoporous titanium dioxide electrode, the ERDs were immobilized adjacent to the IDs via a sequential functionalization approach. In the first step, azidobenzoic acid molecules were co-adsorbed on the mesoporous titanium dioxide surface with the ID. In the second step, the highly selective copper(I)-catalyzed 1,3-dipolar azide-alkyne cycloaddition "click" reaction was employed to couple an alkyne-functionalized ERD to the azidobenzoic acid monolayer. The cycloaddition step in the mesoporous electrode was slowed dramatically due to reactants and catalysts forming agglomerates. In solar cell devices, the close proximity between the surface-immobilized ERD and energy-accepting squaraine sensitizer dyes results in energy transfer efficiencies of up to 91%. The relative improvement in device performance due to the additional ERD spectral response at 124% is among the highest reported. The sequential functionalization approach described herein is transferrable to other applications requiring the functionalization of electrodes with complex molecules.

Introduction

Solar energy conversion in dye-sensitized solar cells (DSCs) occurs at the molecularly functionalized interface of mesoporous titanium dioxide electrodes.[1,2] The photocurrent generated by the solar cell is determined by the spectral response of the sensitizer dye. Energy relay dye (ERD) enhancement of dye-sensitized solar cells has been demonstrated as a pathway to gain panchromatic spectral response in DSCs via Förster resonant energy transfer of photons harvested by the ERD to a surface bonded injection dye (ID).[3–10]

ERDs are usually fluororescent molecules that are introduced into the solar cell by dissolution in the liquid electrolyte[3–6,8] or dispersion in the solid state hole transporter.[9,10] Quantum dots integrated into the meso-porous TiO_2 scaffold are capable of serving as ERDs.[11] Recent reports have had great success depositing ERDs as a second physisorbed layer in quasi solid state DSCs.[12,13] Light harvested by the ERD can enhance the spectral response of the solar cell, if the absorbed photon energy is transferred efficiently to a surface-bonded sensitizer dye that converts absorbed photons into current via injection into the wide-bandgap semiconductor. This sensitizer will therefore be referred to as the injection dye (ID). The quantum efficiency of photons harvested by the ERD therefore also depends on the internal quantum efficiency (IQE) of the ID.

The spectral response from additional ERDs in DSCs is often limited by a low light harvesting efficiency (LHE) due to a limited solubility of the fluorophores in the electrolyte.[3,4,6] More soluble ERD derivatives have been developed but the energy transfer efficiencies (ETEs) were found to become limited both by the formation of non-emissive complexes at high ERD concentrations and quenching of excited ERDs by IDs released from the electrode during device operation.[8]

The ETE between the ERD and ID depends on the Förster radius and distance.[5,14] Supramolecular sensitizers with light harvesting antennas can be considered as examples where the ERD is linked covalently to a surface-bonded sensitizer.[15–19] In quasi solid-state dye sensitized solar cells, physisorption of ERDs on dye-sensitized mesoporous TiO_2 films prior to the deposition of the quasi solid hole transporting medium proved beneficial for high ETEs.[12]

Herein we demonstrate a sequential functionalization approach assembling complex molecules from molecular fragments directly on the mesoporous TiO_2 surface. We

Physical Chemistry Chemical Physics Accepted Manuscript

explored the copper(I)-catalyzed 1,3 dipolar azide-alkyne cycloaddition, referred to as a "click" reaction, for the purpose of covalently linking molecular fragments to each other. This reaction has been utilized previously for the functionalization of various materials including gold,[20,21] allotropes of carbon,[22–24] silica and fluorine-doped tin oxide.[25,26] Within the context of DSCs this reaction has been employed in the synthesis of dyes[27–29] and dyadic energy-transfer compounds.[15,16] However, this is the first demonstration that this reaction can be used to covalently link molecular fragments directly on and inside the confined space of a mesoporous TiO_2 electrode. Non-covalently linked compounds have been demonstrated by association reactions such as ion pairing.[30–32]

The commercial squaraine dye **SQ02** was employed as the ID. This dye requires a co-adsorbant to deaggregate eximers on the TiO_2 surface since these have a lower IQE.[33–35] As co-adsorbants provide logical attachment points for ERDs, 4-azidobenzoic acid (**N_3-BA**) was used as co-adsorbant with **SQ02** in the first sensitization step, illustrated in Figure 1. For this first demonstration, a di-ethynylated pyran fluorophore (**c-DCM**, Figure 2) was synthesized and coupled to the surface-bonded **N_3-BA** via the click reaction forming a triazole bridge between the fragments. By immobilizing the ERD on the mesoporous TiO_2 surface close to the ID, a high light harvesting efficiency by the ERD and high energy transfer efficiency from the ERD to ID of up to 91% was achieved. This resulted in a relative device efficiency increase of up to 124% due to the additional spectral response from the ERD compared to a device comprising no ERD.

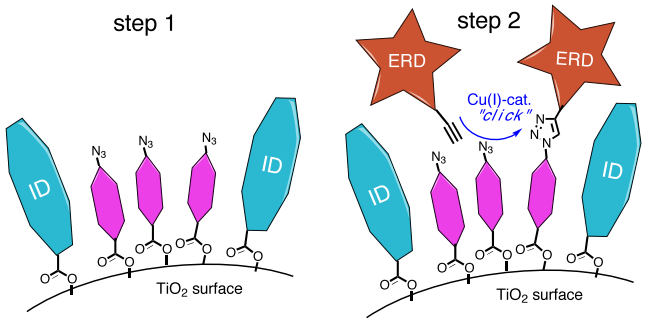

Figure 1: Illustration of the two-step sequential functionalization approach to couple energy relay dyes (ERD) to azide-functionalized co-adsorbers in proximity to energy-accepting injection dyes (ID) on the mesoporous titanium dioxide surface via Cu(I)-catalyzed 1,3-dipolar cycloaddition "click" reaction.

2. Experimental

2.1 Synthesis of an Ethynylated ERD

The di-ethynylated derivative of **DCM**, ((4-(2-(4-(dicyanomethylene)-6-methyl-4*H*-pyran-2-yl)vinyl)phenyl)-azanediyl)bis(ethane-2,1-diyl)bis(pent-4-yno-ate), herein referred to as **c-DCM** (Figure 2), was synthesized in 3 steps in a *ca.* 60% overall yield. Details of the synthetic procedures and characterization of all new compounds are provided in the supporting information. Homogeneous analogues of the anticipated surface-immobilized "clicked" dyes were prepared by reacting **c-DCM** with two equivalents of 4-azidobenzoic acid (**N_3-BA**, TCI America) or its ethyl ester (**N_3-BE**, synthesis described in SI) to form the derivatives **c-DCM-$(BA)_2$** or **c-DCM-$(BE)_2$**, respectively (Scheme 1). For the heterogeneous coupling reaction of **c-DCM**, described in detail in section 2.2, the ratio between molecules coupled to one or two surface-bonded **N_3-BA** molecules could not be determined and this ambiguity is reflected by referring to this compound as **c-DCM-$(BA)_x$-TiO_2** (Scheme 1).

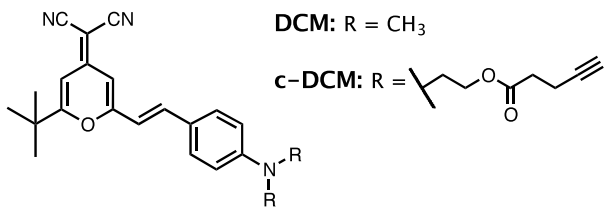

Figure 2: Chemical structure of the energy relay dye **DCM** and its ethyne-functionalized derivative **c-DCM**.

2.2 Two-step functionalization of mesoporous titania

The working electrodes for DSC samples were prepared on conducting fluorine-doped tin oxide (FTO) covered glass (Pilkington, TEC 15). The substrates were rinsed in four consecutive steps using 1) a 10% solution of Extran (Merck) in water, 2) water, 3) acetone and 4) isopropanol, sonicating the substrates for 15 min in each solvent. The mesoporous TiO_2 films were deposited by doctor-blading a commercial paste of TiO_2 with an average nanoparticle diameter of 18 nm (Dyesol NT-18), followed by annealing at 450°C for 30 min. Samples for optical measurements were prepared on microscope slides. The mesoporous TiO_2 film thickness was 5.9 ± 0.4 μm by profilometry. Before dye-sensitization, mesoporous TiO_2 substrates were heated to 450°C for 15 min and left to cool to 70°C before immersion in the dye solution for the first functionalization step (Figure 1). Samples for optical reference measurements were functionalized in 1 mM **N_3-BA** or benzoic acid (**BA**, Sigma-Aldrich) for 8 hrs. Samples for solar cell preparation were immersed in ethanol solutions containing the squaraine sensitizer **SQ02** (0.2 mM)[35,36] and 0 mM, 1 mM, 5 mM, or 10 mM of the co-adsorber **N_3-BA** to vary the ratio between the ID and the surface-binding sites provided by the azido-benzoic acid molecules. Molecules not chemisorbed in this first sensitization step were removed by rinsing with ethanol. For the second step, samples were immersed in solutions containing 1 mM of the "clickable" ERD **c-DCM**, 0.2 mM of the copper(I) catalyst $[Cu(MeCN)_4]SbF_6$, and 0.1 mM triethylamine (NEt_3). The copper(I) catalyst $[Cu(MeCN)_4]SbF_6$ was synthesized by the method of Kubas et al.[37] After this second step, the devices were rinsed with a 10-fold acetonitrile-diluted electrolyte solution to remove unreacted molecules from the porous electrodes (section 3.2), followed by a pure acetonitrile rinse and drying in a nitrogen stream. The undiluted

This journal is © The Royal Society of Chemistry 2012
Physical Chemistry Chemical Physics Accepted Manuscript

electrolyte solution contained 600 mM 1-methyl-3-propylimidazolium iodide, 40 mM I_2, 280 mM 4-tert-butylpyridine, 25 mM LiI and 50 mM guanidinium thiocyanate in a 15:85 (by volume) mixture of valeronitrile and acetonitrile.

Optical spectra were collected on a Cary 6000i UV/Vis spectrophotometer. Fluorescence spectra were measured using a Horiba Jobin-Yvon Spex Fluorolog-3 fluorometer equipped with a 450W Xenon lamp (230-1800 nm excitation) in combination with a monochromator with a thermoelectrically cooled R928P detector (240-850 nm). Solution samples were measured using the right angle and solid-state samples were measured in front-face mode with the incident beam perpendicular to the surface of the slide. Unless noted otherwise, the excitation wavelength for the emission spectra was 450 nm.

2.3 Dye-sensitized solar cell fabrication and testing

Solar cell devices were manufactured by assembling the sequentially functionalized mesoporous TiO_2 films on FTO glass substrates with platinized FTO counter electrode using a 25 μm thick meltable surlyn (Solaronix) frame and a commercial T-Shirt heat press to melt the two electrodes together. The electrolyte solution was vacuum back-filled through a hole drilled into the counter-electrode that was sealed consecutively with a small piece of surlyn and a glass cover slip.

Current-voltage measurements were carried out using a Keithley 2400 potentiometer under simulated AM1.5G illumination using a Spectraphysics model 91160 solar simulator. The light intensity was calibrated to be 1000 W m^{-2} using a Hamamatsu Si photodiode with KG5 filter. The active working electrode area of 0.25 cm^2 was masked during measurements. The external quantum efficiency (EQE) of solar cell devices was measured using a setup described elsewhere.[8] The energy transfer efficiency (ETE) from the energy relay dye (ERD) to the injection dye (ID) was estimated by determining the light harvesting efficiency (LHE) of both dyes in the devices using an integrating sphere, accounting for reflection and parasitic absorption losses, as described elsewhere.[4,8]

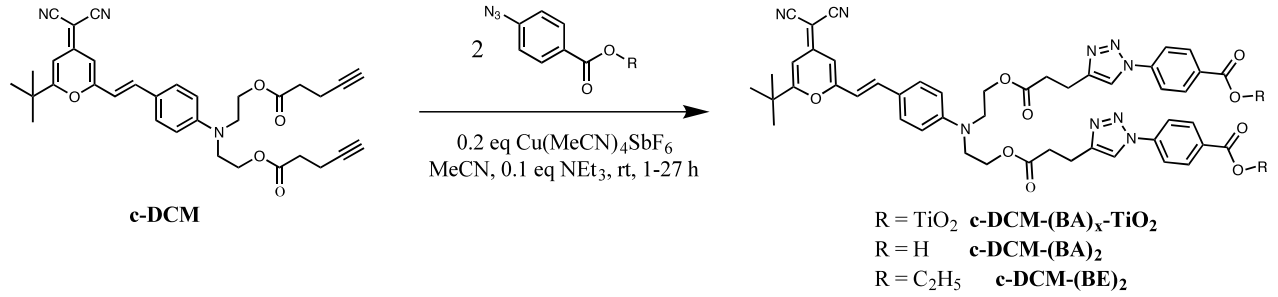

Scheme 1: Heterogeneous reaction scheme in which the ethynylated energy relay dye (**c-DCM**) is linked to surface-bonded 4-azidobenzoic acid on mesoporous TiO_2 (R = TiO_2). For reference, **c-DCM** was homogeneously coupled to 4-azidobenzoic acid (R = H) and 4-azidobenzoic acid ethyl ester (R = C_2H_5), referred to as **c-DCM-(BA)$_2$** and **c-DCM-(BE)$_2$**, respectively.

3. Results and Discussion

3.1 DCM derivative synthesis and spectral overlap with SQ02

The homogeneously-coupled di-carboxylic acid derivative of the clickable energy relay dye, **c-DCM-(BA)$_2$** (Scheme 1), proved to be very insoluble. Attempts to immobilize this dye on mesoporous TiO_2 films from any dilute solution resulted in significantly lower amounts of adsorbed **c-DCM-(BA)$_2$** compared to the two-step method (Figure S7). An intended comparison of the two step immobilization procedure with a co-sensitization approach was therefore not feasible. Solubility issues of complex functional molecules are avoided in the sequential functionalization presented herein.

The optical (Figure S8) and electrochemical (Figure S9) properties of **c-DCM** and **c-DCM-(BE)$_2$** (Scheme 1) were comparable to **DCM** and are summarized in Table 1. The negligible differences between the **DCM** derivatives indicates that the conjugation of the **DCM** chromophore does not extend appreciably into the anchoring fragment through the triazole and ester bridges. This lack of conjugation inhibits direct photo-induced charge transfer from the ERD into mesoporous TiO_2 and photocurrent generation from the ERD in absence of an ID was found to be insignificant.

Comparing the normalized absorption and emission spectra of surface-bonded **c-DCM-(BA)$_x$-TiO$_2$** and **SQ02-ZrO$_2$** shows significant spectral overlap between the **c-DCM-(BA)$_x$-TiO$_2$** emission and **SQ02** absorption (Figure 3). The absorption and emission spectrum of **SQ02** was measured for the dye bonded to ZrO_2 and co-adsorbed with 10 mM **N$_3$-BA** to avoid quenching of the photoluminescence by electron injection into TiO_2. The Förster radius (R_0) for the surface-bonded **c-DCM-(BA)$_x$-TiO$_2$** and **SQ02-ZrO$_2$** was calculated as described elsewhere and found to be 6.1 nm.[4] This is comparable to other ERD/ID couples such as the **DCM** fluorophore and the ID **TT1**.[4] Due to the large R_0 and close proximity of the surface-

Physical Chemistry Chemical Physics Accepted Manuscript

bonded **c-DCM** to the ID **SQ02**, energy transfer is predicted to be efficient.

Table 1: Comparison of optical and electronic properties of dyes

Compound	ε_r^a ($M^{-1}cm^{-1}$)	Abs_{max}^b (nm)	E_{ox}^c (V *vs* Fc)	$E_{A\text{-}PL}^d$ (eV)
DCM	44 900[e]	460[e]		2.22
c-DCM	39 000	475	0.55	2.25
c-DCM(BE)$_2$	43 000	475	0.58	2.24
SQ02	319 000[f]	662[f]	0.22[f]	1.81[f]

[a]Extinction coefficient, [b]Absorption maximum, [c]Oxidation potential with respect to ferrocene (Fc) reference deteremined from the half-wave potential in cyclic voltammentry measurements [d]Intercept of normalized absorption and emission spectra, as an estimate for the bandgap of the dyes, [e]Literature values from ref [4], [f]Literature values from ref [34].

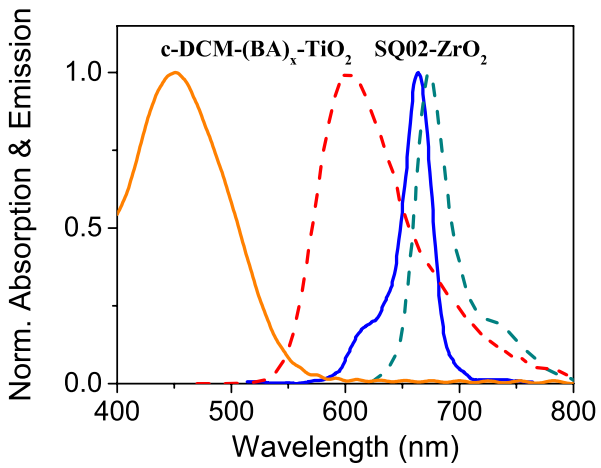

Figure 3: Comparison of the absorption (solid) and emission (dashed) spectra of **c-DCM-(BA)$_x$** bonded to mesoporous TiO_2 (absorption, orange, solid; emission, red, dashed) and **SQ02** bonded to mesoporous ZrO_2 (absorption, blue, solid; emission, turquois, dashed). The energy transfer efficiency depends on the spectral overlap between **c-DCM-(BA)$_x$-TiO$_2$** emission and **SQ02** absorption.

3.2 Cu(I)-catalyzed click functionalization step

The second functionalization step in which **c-DCM** is coupled to the surface-bonded **N$_3$-BA** via Cu(I) catalyzed 1,3-dipolar cycloaddition was found to be slow. Reaction times of more than 24 hrs at room temperature are necessary to achieve high surface loadings of **c-DCM**. We found this slow rate for the ERD immoblization was caused by slow diffusion of reactants within the mesoporous electrodes.

In the first attempts to make solar cell devices for this study, the device performance was low. While absorptance measurements suggested considerable deposition of the ERD onto the electrodes during the second functionalization step and high LHE of the ID, a low spectral response from both the ERD and ID suggested insufficient conversion of absorbed photons into current and thus a low IQE of the ID. After 3 days of storage, the device performance increased 10-fold and color of the electrolyte solution adjacent to the active area of the solar cell devices suggested partial dissolution of ERDs. We therefore investigated the possibility of ERD agglomerates within the mesoporous electrode during the second functionalization step as the cause of the low IQE. As the ionic environment of the electrolyte seemed to attenuate this pore clogging issue, a rinsing step with diluted electrolyte solution was introduced (section 2.2).

The spectra of a **N$_3$-BA** functionalized 6-µm-thick mesoporous TiO_2 electrode after immersion in the click-reaction solution for 27 hrs and rinsed with pure acetonitrile (MeCN) or diluted electrolyte solution are compared in Figure 4. The absorbance difference of 1.2 units at 450 nm illustrates that an acetonitrile rinse alone is inefficient in removing weakly associated or agglomerated dyes. In control experiments, benzoic acid (**BA**) functionalized mesoporous TiO_2 were subjected to the second functionalization step. The absorbance difference of ca. 1.2 absorbance units between the acetonitrile-rinsed and electrolyte-rinsed sample shows that a comparable amount of **c-DCM** is deposited onto the electrodes even without azide groups. The negligible absorbance from **c-DCM** after electrolyte rinsing proves that the Cu(I)-catalyzed coupling reaction is indeed selective to azide-functionalized molecules and a considerable amount of **c-DCM** becomes trapped within the mesoporous electrodes in the click-reaction step. The diluted electrolyte rinse is effective at dissolving agglomerated reactants from the mesoporous electrodes.

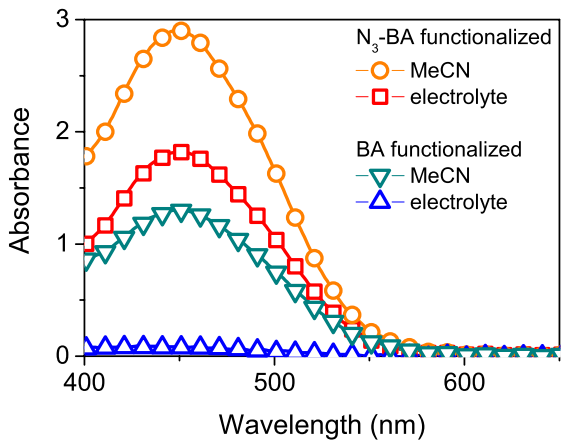

Figure 4: Absorbance of mesoporous titania samples (6 µm) functionalized with 4-azidobenzoic acid (**N$_3$-BA**) and benzoic acid (**BA**) followed by click-functionalization with **c-DCM**. The electrodes were rinsed with either MeCN or the diluted electrolyte solution.

3.3. Solar cell device results

A series of sequentially functionalized solar cell devices were prepared varying both the **N$_3$-BA** concentration in the first sensitization step from 1 to 5 and 10 mM and the duration of the second, cycloaddition reaction step from 0 to 27 hrs. From changes in the **SQ02** absorbance and the characteristic differences in the EQE of **SQ02** sensitized solar cells with varying amount of additional co-adsorber in Figure 5a, the addition of **N$_3$-BA** to the sensitization solution was found to reduce the degree of dye aggregation in a similar manner to the

This journal is © The Royal Society of Chemistry 2012
Physical Chemistry Chemical Physics Accepted Manuscript

commonly used co-adsorber cheno-deoxycholic acid. This is evident in the reduction of the H-aggregate shoulder at *ca*. 600 nm (Figure S11).[34–36,38] The EQE of **SQ02**-sensitized solar cell devices prepared with 10 mM cheno-deoxycholic acid is compared in Figure 5a.[38] **SQ02** without additional co-adsorber exhibits a low IQE despite a high LHE due to inefficient electron injection from **SQ02** eximers.[34,38]

The solar cell device performance metrics derived from photocurrent-density-voltage (*J-V*) measurements are summarized in Table 2. For all concentrations of **N_3-BA**, an increase of the device fill factor (FF) is observed after the **c-DCM** is introduced in the second functionalization step. This indicates that the additional layer of organic molecules on the mesoporous TiO_2 surface helps to prevent charge carrier recombination between photo-injected electrons in TiO_2 with species in the electrolyte as reported elsewhere.[12] This is further supported with the concomitant increase in the open-circuit voltage, V_{OC}. For the device prepared using 10 mM of **N_3-BA** in the first sensitization step, the relative improvement in device efficiency due to the additional response from an ERD is 124%. This increase is the highest relative improvement due to the additional photocurrent generated by an ERD reported to date (Table S1).

From the measured LHE differences determined for full devices (Figure S12), the amount of immobilized **c-DCM** depends on the relative amount of surface binding sites as well as the reaction time in the second functionalization step. This is illustrated in Figure 6. The increase in LHE with reaction time is accompanied clearly by an increased spectral response between 400-550 nm (Figure 5a-c) and increase in J_{sc} of the solar cell devices, accordingly (Table 2). For the devices using the lowest **N_3-BA** concentration of 1 mM, the photocurrent does not increase significantly (Table 2). Apparent from the EQE measurements (Figures 5a-c), the slight increase in spectral response from the ERD is offset by a reduction in spectral response from the **SQ02** ID. The reduction of spectral response from the ID for this case suggests a detrimental effect of the click reaction conditions on the IQE of SQ02. We speculate here that the regeneration efficiency is decreased. Because of the lower redox potential of the ERD with respect to the ID, hole trapping on the ERD is unlikely; however, steric inhibition of the redox couple to the TiO_2 surface for regeneration of the ID is possible.

Table 2: Solar Cell Device Figures of Merit.

$[N_3\text{-BA}]^a$ (mM)	Reaction time (hrs)	$J_{SC}{}^b$ (mA cm^{-2})	$V_{OC}{}^c$ (V)	FF^d	η^e (%)
1	0	3.72	0.64	0.63	1.49
	10	4.02	0.61	0.75	1.84
	27	3.42	0.64	0.76	1.69
5	0	3.87	0.64	0.71	1.79
	10	4.60	0.65	0.77	2.33
	27	5.81	0.66	0.75	2.88
10	0	2.85	0.63	0.71	1.29
	10	4.48	0.65	0.77	2.26
	27	5.60	0.67	0.77	2.89

[a]Concentration of azidobenzoic acid in the **SQ02** dye solution [b]Short-circuit current [c]Open-circuit voltage [d]Fill Factor [e]Device efficiency

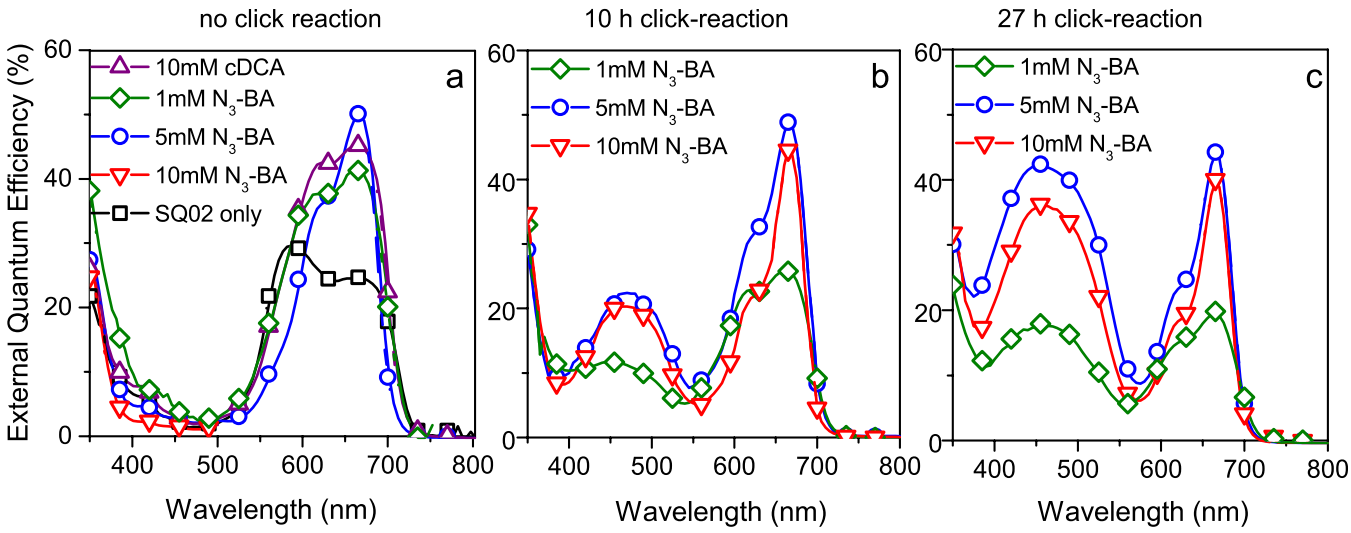

Figure 5: Comparison of external quantum efficiency measurements for devices with different amount of co-adsorbed **N_3-BA** (diamonds 1 mM, circles 5mM and triangles 10 mM) subjected to the cyclization reaction conditions for different amounts of time: a) 0 min (references), b) 10 hrs and c) 27 hrs. The EQE for **SQ02** (squares) without any co-adsorber and with 10 mM added cheno-deoxycholic acid (triangels facing up) were added to plot a for comparison.

Physical Chemistry Chemical Physics Accepted Manuscript

Journal Name RSCPublishing

ARTICLE

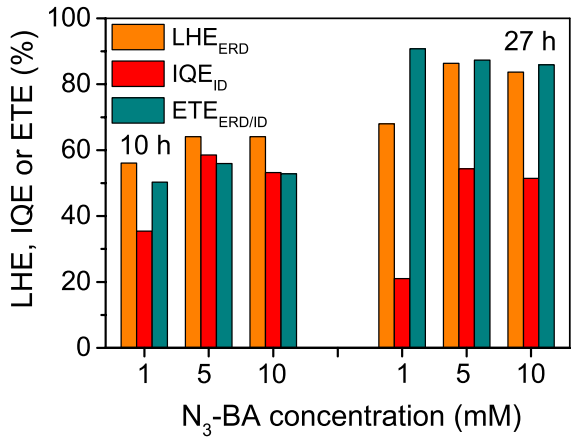

Figure 6: Light harvesting efficiency of the ERD (LHE_{ERD}), internal quantum efficiency of the ID (IQE_{ID}) and resulting energy transfer efficiency from the ERD to ID ($ETE_{ERD/ID}$) as a function of N_3-BA solution concentration during sensitization and click-reaction time.

For the device prepared with 5 mM **N_3-BA** the maximum peak in the EQE near 660 nm generated by the ID remains similar but the spectral response from the H-aggregate shoulder near 600 nm decreases (Figure 5a-c). This indicates some desorption but also reduced aggregation of **SQ02** during the second functionalization step. The increase in J_{SC} (Table 2) due to the additional spectral response from the ERD is therefore slighly offset by a reduction in photocurrent generated from the ID.

Devices made from photoanodes sensitized with 10 mM **N_3-BA** as co-adsorbant in the first functionalization step exhibit a spectral response from the **SQ02** ID that remains almost unchanged (Figure 5a-c). The relative increase in J_{SC} due to the additional spectral response from the ERD is therefore the highest for all devices compared in this study. With the increase in V_{OC} and FF, the overall relative device efficiency increases 124% compared to devices made from electrodes exposed to the second functionalization for 27 h with the reference device that was not exposed to the click reaction (Table 2).

3.4. Energy transfer efficiency

The energy transfer efficiency from the ERD to the ID ($ETE_{ERD/ID}$) can be estimated from the external quantum efficiency response of the energy relay dye (EQE_{ERD}) divided by the light harvesting efficiency of the ERD (LHE_{ERD}) and the internal quantum efficiency of the ID (IQE_{ID}) as described elsewhere.[4,8] The LHE_{ERD} was determined from the absorptance of full devices, accounting for parasitic absorption losses in the electrodes, mp-TiO_2, and electrolyte (Figure S12). The IQE_{ID} was determined from the EQE_{ID} and LHE_{ID} (Figure S12). In Figure 6, the respective values for LHE_{ERD}, IQE_{ID} and the resulting $ETE_{ERD/ID}$ are compared for the shorter (10 h) and longer (27 h) click-reaction times. The increase in LHE_{ERD} at the longer reaction time reflects the increase of immobilized **c-DCM**.

As discussed in section 3.2, the second functionalization step becomes increasingly diffusion limited as reactant agglomerates form inside the mesoporous electrode. The ERD concentration is therefore expected to be higher in the uppermost region of the mesoporous TiO_2 film while longer reaction times allow the ERD and catalyst to diffuse to sites closer to the FTO front contact in the solar cell device.[39] The more even distribution of ERD throughout the whole mesoporous electrode after 27 h results in an increase of the average $ETE_{ERD/ID}$ from ca. 50% to an average of 88%. The $ETE_{ERD/ID}$ is the highest (91%) for devices constructed with the lowest **N_3-BA** concentration and decreased slightly to 87% and 86% for **N_3-BA** concentrations of 5 mM and 10 mM, respectively. This slight decrease in $ETE_{ERD/ID}$ with increasing **N_3-BA** surface binding sites is indicative of a longer average distance between the ID and ERD as the relative surface concentration of ID is reduced. In photoluminescence measurements of mesoporous ZrO_2, samples functionalized prepared using the sequential functionalization approach described here, an increase in residual photoluminescence from the ERD was observed with increasing concentration of **N_3-BA** and hence ERD surface concentration (Figure S13). Further studies are necessary to determine the limit of the ERD to ID surface ratio for efficient energy transfer.

The ETE for the surface immobilized ERD approach is among the highest reported. These values are comparable to dyadic ERD-ID compounds[7,40] and the highest value achieved for an electrolyte-dissolved ERD-enhanced DSC device.[4]

Conclusions and Outlook

Surface-immobilization is a beneficial strategy to reduce the energy relay dye (ERD) to injection dye (ID) distance and thus increase the energy transfer efficiency (ETE) in ERD-enhanced dye-sensitized solar cells. ETEs of up to 91% were achieved. Comparing relative device efficiency improvements due to the additional spectral response from an ERD, the maximum achieved relative improvement of 124% is the highest reported to date (Table S1).

This report demonstrates the viability of modifying mesoporous electrodes using coupling reactions to form complex, functional molecules from their constituent fragments. The Cu(I) catalyzed 1,3-dipolar azide-alkyne

Physical Chemistry Chemical Physics Accepted Manuscript

cycloaddition reaction, used in this report to couple alkyne-functionalized ERDs to azidobenzoic acid molecules bonded to mesoporous titanium dioxide, was chemoselective. During the coupling step, reactant agglomerates formed within the mesoporous electrodes, which proved determintal to both the reaction rate as well as solar cell device performance. Alternative coupling reactions, such as catalyst-free strain-promoted click-chemistry, need to be explored to avoid this problem. Performing the second functionalization step under continuous flow of the reactant solutions or in an electrolyte solution could potentially increase reaction rates as well.[41,42]

Herein, the sequential functionalization approach was explored to increase the LHE of ERDs in ERD-enhanced DSCs. We believe that this approach will be beneficial to other applications involving the functionalization of mesoporous electrodes with large, complex molecules. By assembling the fragments of these molecules directly on the electrode surface, the purification and isolation of large, insoluble molecules can be avoided. Building upon the approach discussed herein, ERDs can be coupled directly to IDs to form molecular diads.[7,40] In this case, ERDs will be situated in an outer sphere of the first molecular layer without occupying space at the TiO_2 interface.

Acknowledgements

E. L. U. thanks the Marcus and Amalia Wallenberg memorial fund for a postdoctoral scholarship. S. J. F. thanks the Center for Molecular Analysis and Design (CMAD) in the Department of Chemistry at Stanford University for a graduate fellowship. Funding for this collaborative project was provided by the Precourt Institute at Stanford University.

Notes and references

[a] Department of Materials Science and Engineering, Stanford University, USA

[b] Department of Chemistry, Stanford University, USA.

[†]Present address: Eva Unger, Department of Chemistry, Lund University, Box 124, 221 00 Lund, Sweden e-mail: eva.unger@chemphys.lu.se

Electronic Supplementary Information (ESI) available: Synthetic details, structural, optical, and electrochemical characterization of DCM compounds presented herein. Chemisorption measurements of **c-DCM-(BA)$_2$** to mesoporous titania. First batch of devices indicating pore clogging after click reaction conditions. Absorption of **SQ02** as a function of **N$_3$-BA** concentration. Light harvesting efficiency of solar cell devices. Compilation of reported solar cell efficiency data. Photoluminescence reference measurements on mesoporous zirconia films. This information is available free of charge. See DOI: 10.1039/b000000x/

References

1. B. O'Regan and M. Grätzel, *Nature*, 1991, **353**, 737–740.
2. A. Hagfeldt, G. Boschloo, L. Sun, L. Kloo, and H. Pettersson, *Chem. Rev.*, 2010, **110**, 6595–663.
3. B. E. Hardin, E. T. Hoke, P. B. Armstrong, J.-H. Yum, P. Comte, T. Torres, J. M. J. Fréchet, M. K. Nazeeruddin, M. Grätzel, and M. D. McGehee, *Nat. Photonics*, 2009, **3**, 406–411.
4. B. E. Hardin, J.-H. Yum, E. T. Hoke, Y. C. Jun, P. Péchy, T. Torres, M. L. Brongersma, M. K. Nazeeruddin, M. Grätzel, and M. D. McGehee, *Nano Lett.*, 2010, **10**, 3077–83.
5. E. T. Hoke, B. E. Hardin, and M. D. McGehee, *Opt. Express*, 2010, **18**, 3893–904.
6. J.-H. Yum, B. E. Hardin, E. T. Hoke, E. Baranoff, S. M. Zakeeruddin, M. K. Nazeeruddin, T. Torres, M. D. McGehee, and M. Grätzel, *Chemphyschem*, 2011, **12**, 657–61.
7. C. Siegers, J. Hohl-Ebinger, B. Zimmermann, U. Würfel, R. Mülhaupt, A. Hinsch, and R. Haag, *Chemphyschem*, 2007, **8**, 1548–56.
8. G. Y. Margulis, B. Lim, B. E. Hardin, E. L. Unger, J.-H. Yum, J. M. Feckl, D. Fattakhova-Rohlfing, T. Bein, M. Grätzel, A. Sellinger, and M. D. McGehee, *Phys. Chem. Chem. Phys.*, 2013, **15**, 11306–12.
9. J.-H. Yum, B. E. Hardin, S.-J. Moon, E. Baranoff, F. Nüesch, M. D. McGehee, M. Grätzel, and M. K. Nazeeruddin, *Angew. Chem. Int. Ed. Engl.*, 2009, **48**, 9277–80.
10. G. K. Mor, J. Basham, M. Paulose, S. Kim, O. K. Varghese, A. Vaish, S. Yoriya, and C. A. Grimes, *Nano Lett.*, 2010, **10**, 2387–94.
11. S. Buhbut, S. Itzhakov, E. Tauber, M. Shalom, I. Hod, T. Geiger, Y. Garini, D. Oron, and A. Zaban, *ACS Nano*, 2010, **4**, 1293–8.
12. R. Gao, Y. Cui, X. Liu, and L. Wang, *Sci. Rep.*, 2014, **4**, 5570.
13. H. J. Yun, D. Y. Jung, D. K. Lee, A. K.-Y. Jen, and J. H. Kim, *Dye. Pigment.*, 2015, **113**, 675–681.
14. N. D. Eisenmenger, K. T. Delaney, V. Ganesan, G. H. Fredrickson, and M. L. Chabinyc, *J. Phys. Chem. C*, 2014, **118**, 14098–14106.
15. R. Schütz, S. Malhotra, I. Thomas, C. Strothkämper, A. Bartelt, K. Schwarzburg, T. Hannappel, C. Fasting, and R. Eichberger, *J. Phys. Chem. C*, 2014, **118**, 9336–9345.
16. R. Eichberger, C. Strothkämper, I. Thomas, T. Hannappel, K. Schwarzburg, C. Fasting, A. Bartelt, and R. Schütz, *J. Photonics Energy*, 2012, **2**, 021003.
17. J. Warnan, F. Buchet, Y. Pellegrin, E. Blart, and F. Odobel, *Org. Lett.*, 2011, **13**, 3944–7.
18. J. Warnan, Y. Pellegrin, E. Blart, and F. Odobel, *Chem. Commun. (Camb).*, 2012, **48**, 675–7.
19. J. Warnan, J. Gardner, L. Le Pleux, J. Petersson, Y. Pellegrin, E. Blart, L. Hammarström, and F. Odobel, *J. Phys. Chem. C*, 2014, **118**, 103–113.
20. J. P. Collman, N. K. Devaraj, and C. E. D. Chidsey, *Langmuir*, 2004, **20**, 1051–1053.
21. N. K. Devaraj, G. P. Miller, W. Ebina, B. Kakaradov, J. P. Collman, E. T. Kool, and C. E. D. Chidsey, *J. Am. Chem. Soc.*, 2005, **127**, 8600–1.
22. A. Devadoss and C. E. D. Chidsey, *J. Am. Chem. Soc.*, 2007, **129**, 5370–1.
23. E. D. Stenehjem, V. R. Ziatdinov, T. D. P. Stack, and C. E. D. Chidsey, *J. Am. Chem. Soc.*, 2013, **135**, 1110–6.
24. R. E. Ruther, M. L. Rigsby, J. B. Gerken, S. R. Hogendoorn, E. C. Landis, S. S. Stahl, and R. J. Hamers, *J. Am. Chem. Soc.*, 2011, **133**, 5692–4.
25. M. A. Pellow, T. D. P. Stack, and C. E. D. Chidsey, *Langmuir*, 2013, **29**, 5383–7.

Physical Chemistry Chemical Physics Accepted Manuscript

26. M. C. Benson, R. E. Ruther, J. B. Gerken, M. L. Rigsby, L. M. Bishop, Y. Tan, S. S. Stahl, and R. J. Hamers, *ACS Appl. Mater. Interfaces*, 2011, **3**, 3110–9.
27. T. Duan, K. Fan, Y. Fu, C. Zhong, X. Chen, T. Peng, and J. Qin, *Dye. Pigment.*, 2012, **94**, 28–33.
28. I. Stengel, A. Mishra, N. Pootrakulchote, S.-J. Moon, S. M. Zakeeruddin, M. Grätzel, and P. Bäuerle, *J. Mater. Chem.*, 2011, **21**, 3726.
29. I. Stengel, N. Pootrakulchote, R. R. Dykeman, A. Mishra, S. M. Zakeeruddin, P. J. Dyson, M. Grätzel, and P. Bäuerle, *Adv. Energy Mater.*, 2012, **2**, 1004–1012.
30. P. K. D. D. P. Pitigala, M. K. I. Seneviratne, V. P. S. Perera, and K. Tennakone, *Langmuir*, 2004, **20**, 5100–5103.
31. J.-F. Gnichwitz, R. Marczak, F. Werner, N. Lang, N. Jux, D. M. Guldi, W. Peukert, and A. Hirsch, *J. Am. Chem. Soc.*, 2010, **132**, 17910–20.
32. B. A. Putans, L. M. Bishop, and R. J. Hamers, *Chem. Mater.*, 2014, **26**, 3651–3659.
33. J.-H. Yum, S.-R. Jang, R. Humphry-Baker, M. Grätzel, J.-J. Cid, T. Torres, and M. K. Nazeeruddin, *Langmuir*, 2008, **24**, 5636–40.
34. T. Geiger, S. Kuster, J.-H. Yum, S.-J. Moon, M. K. Nazeeruddin, M. Grätzel, and F. Nüesch, *Adv. Funct. Mater.*, 2009, **19**, 2720–2727.
35. E. L. Unger, A. Morandeira, M. Persson, B. Zietz, E. Ripaud, P. Leriche, J. Roncali, A. Hagfeldt, and G. Boschloo, *Phys. Chem. Chem. Phys.*, 2011, **13**, 20172–7.
36. E. Unger, Uppsala University, 2012.
37. G. J. Kubas, B. Monzyk, and A. L. Crumbliss, *Inorganic Synthesis*, John Wiley & Sons, Inc., Hoboken, NJ, USA, 1979, vol. 19.
38. J. H. Yum, S. J. Moon, R. Humphry-Baker, P. Walter, T. Geiger, F. Nüesch, M. Grätzel, and M. D. K. Nazeeruddin, *Nanotechnology*, 2008, **19**, 424005.
39. B. O'Regan, L. Xiaoe, and T. Ghaddar, *Energy Environ. Sci.*, 2012, **5**, 7203.
40. C. Siegers, U. Würfel, M. Zistler, H. Gores, J. Hohl-Ebinger, A. Hinsch, and R. Haag, *Chemphyschem*, 2008, **9**, 793–8.
41. P. J. Holliman, M. L. Davies, A. Connell, B. Vaca Velasco, and T. M. Watson, *Chem. Commun. (Camb).*, 2010, **46**, 7256–8.
42. P. J. Holliman, M. Mohsen, A. Connell, M. L. Davies, K. Al-Salihi, M. B. Pitak, G. J. Tizzard, S. J. Coles, R. W. Harrington, W. Clegg, C. Serpa, O. H. Fontes, C. Charbonneau, and M. J. Carnie, *J. Mater. Chem.*, 2012, **22**, 13318.

This journal is © The Royal Society of Chemistry 2012

Physical Chemistry Chemical Physics Accepted Manuscript